https://doi.org/10.46344/JBINO.2026.v15i01.23

"ULTRASOUND-RESPONSIVE PLGA NANOBUBBLES FOR IMPROVED ORAL BIOAVAILABILITY OF ENZALUTAMIDE: FORMULATION OPTIMIZATION AND PHARMACOKINETIC EVALUATION"

K.Narendra*,Dr.AmitKumar1,Kokkula Pavan Kumar[2]

*Research Scholar, Faculy of Pharmaceutical Sciences,MotherhoodUniversiy,Roorkee,247661

[1]Research Supervisor, Faculy of Pharmaceutical Sciences,MotherhoodUniversiy,Roorkee, 247661

[2]Associate Professor, , Faculty of Pharmaceutical Sciences, Motherhood University, Roorkee, 247661

Abstract

Poor aqueous solubility and low oral bioavailability limit the therapeutic effectiveness of enzalutamide, a second-generation androgen receptor inhibitor used in advanced prostate cancer. This study aimed to develop and optimize ultrasound-responsive PLGA nanobubbles to enhance oral delivery and pharmacokinetic performance. Nanobubbles were prepared using the solvent evaporation method and optimized via a Box–Behnken design, evaluating the effect of formulation variables on key quality attributes. The optimized formulation exhibited a particle size of 193.5 ± 2.8 nm, polydispersity index of 0.26 ± 0.016, zeta potential of −31.4 ± 1.17 mV, and entrapment efficiency of 65.12 ± 2.54%. Characterization by FTIR, DSC, and XRD confirmed drug–polymer compatibility, and SEM revealed uniform spherical morphology. In vitro studies showed sustained and ultrasound-triggered drug release. In vivo evaluation in Wistar rats demonstrated significant increases in C_max and AUC_0–t, confirming enhanced oral absorption and prolonged systemic exposure. These results indicate that ultrasound-responsive PLGA nanobubbles are a promising oral delivery platform for poorly soluble anticancer drugs.

Key words:PLGA nanobubbles; Enzalutamide; Ultrasound-responsive drug delivery; Oral bioavailability; Anticancer drug delivery; Box–Behnken design; Pharmacokinetics

1.Introduction

Prostate cancer remains one of the most frequently diagnosed malignancies among men worldwide and continues to pose a major clinical challenge due to disease progression, therapeutic resistance, and limitations associated with conventional treatment strategies. Although androgen deprivation therapy represents the cornerstone of management for advanced prostate cancer, resistance to first-generation anti-androgens frequently develops, necessitating the use of more potent agents such as enzalutamide. Enzalutamide, a second-generation androgen receptor signalling inhibitor, has demonstrated significant clinical benefits in metastatic and castration-resistant prostate cancer. However, its therapeutic performance following oral administration is severely compromised by poor aqueous solubility, extensive first-pass metabolism, and limited bioavailability, which require high dosing and may increase the risk of adverse effects.

Nanotechnology-based drug delivery systems have emerged as promising tools to overcome pharmacokinetic and biopharmaceutical limitations of poorly soluble anticancer drugs. Polymeric nanocarriers, particularly those composed of poly(lactic-co-glycolic acid) (PLGA), have attracted considerable attention owing to their biodegradability, biocompatibility, controlled drug release properties, and regulatory acceptance. While nanoparticles, microspheres, and liposomes have been widely investigated, nanobubbles represent a relatively novel class of nanocarriers characterized by a gas-filled core surrounded by a stabilizing polymeric shell. Their unique structural features confer high surface area, improved stability, and responsiveness to external stimuli such as ultrasound.

Ultrasound has been extensively explored as a non-invasive and clinically acceptable modality to enhance drug delivery. When applied to nanobubble systems, ultrasound induces cavitation phenomena that can transiently increase membrane permeability and trigger controlled drug release at the target site. This ultrasound-responsive behavior offers a distinct advantage over conventional nanocarriers by enabling spatiotemporal control of drug release, thereby improving therapeutic efficacy while minimizing systemic exposure. Despite these advantages, most nanobubble-based drug delivery studies have primarily focused on parenteral or imaging applications, with limited exploration of their potential for oral drug delivery.

Oral administration remains the most preferred route for chronic cancer therapy due to improved patient compliance and ease of administration. However, the development of effective oral delivery systems for hydrophobic anticancer drugs remains a significant challenge. Nanobubbles, owing to their nanoscale size and enhanced stability, may facilitate improved gastrointestinal absorption and prolonged systemic circulation. Moreover, the integration of ultrasound-mediated release mechanisms with oral nanobubble formulations represents an underexplored strategy with substantial potential to improve bioavailability and pharmacokinetic performance.

In this context, the present study aimed to develop and optimize ultrasound-responsive PLGA nanobubbles for the oral

delivery of enzalutamide. A systematic formulation approach based on Box–Behnken design was employed to optimize critical formulation and process variables. The optimized nanobubbles were extensively characterized for physicochemical properties, in vitro release behavior under ultrasound stimulation, and in vivo pharmacokinetic performance. This work seeks to establish PLGA nanobubbles as a promising oral drug delivery platform for poorly soluble anticancer agents and to provide mechanistic insights into ultrasound-triggered enhancement of drug bioavailability.

1.2Fundamentals of Nanobubbles: Nanobubbles (NBs) exhibit remarkable stability, strong affinity for hydrophobic surfaces, and prolonged persistence in aqueous systems. These unique properties enable their broad application across diverse fields, including surface coating and cleaning, pollution remediation, energy systems, medicine, fluidics, agriculture, and metabolic enhancement in plant and animal systems (Benezra et al., 2011). Over the past two decades, interest in nanobubble technology has increased substantially due to rapid technical advancements. Market projections estimated the European nanobubble industry to reach €145 million by 2030, while recent global analyses suggest a multi-billion-dollar valuation, with water and wastewater treatment emerging as the dominant application area. Expanding adoption is also evident in energy, agriculture, and biomedical sectors (Bernards et al., 2023).

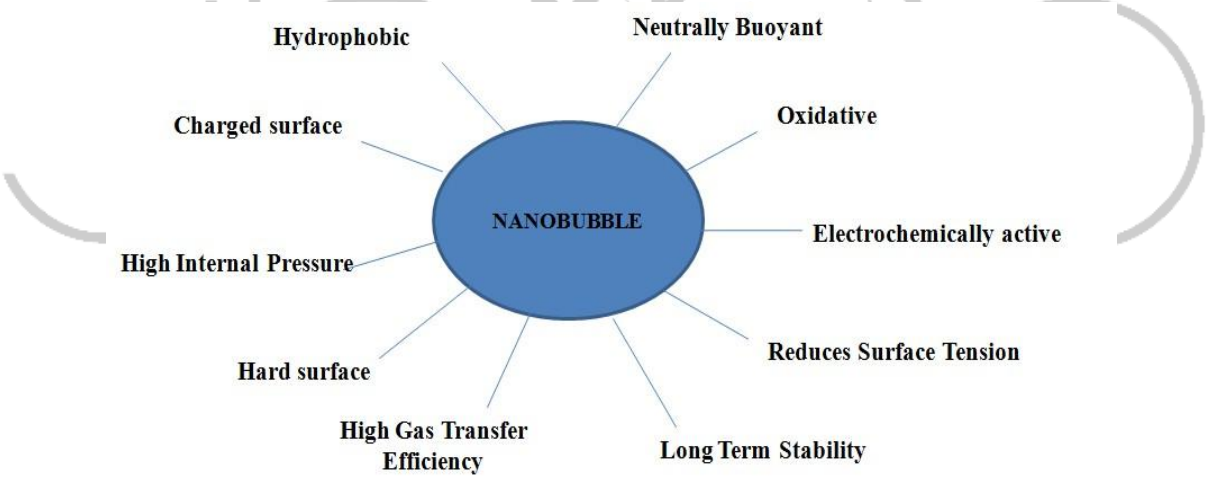

Figure: Fundamentals of NBs

1.3.Composition Membrane and Non-Membrane of Nanobubbles:

Membrane nanobubbles (NBs) consist of three components: a gas core, a shell layer, and a surrounding liquid phase. The shell, typically composed of surfactants, polymers, or lipids, stabilizes the gas core by limiting gas diffusion, thereby contributing to long-term stability . In contrast, non-membrane NBs comprise only a gas core and liquid phase. Although classical theory predicts reduced stability with decreasing bubble size, non-membrane NBs exhibit unexpected stability despite the absence of a protective shell (Chen et al., 2014; Bray et al., 2021).

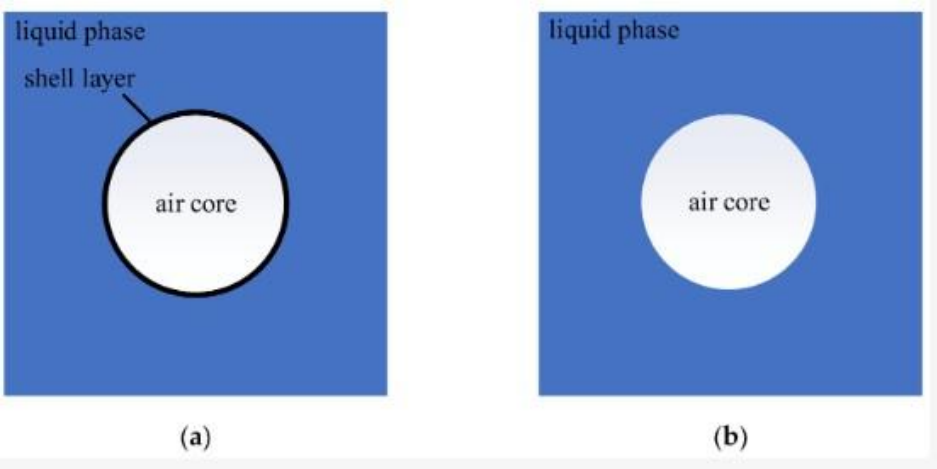

Figure: Nanobubble structure diagram:
(a) membrane NBs; (b) non-membrane NBs

1.4 Applications of Nanobubbles

Nanobubbles (NBs), also known as ultrafine bubbles, are widely used due to their unique stability, high surface area, and responsiveness to external energy. In medicine, NBs serve as ultrasound contrast agents and drug delivery carriers, produced using microfluidic or nanoporous membrane techniques to ensure precise size control. In agriculture, simpler preparation methods are sufficient, where NBs enhance plant growth by increasing dissolved oxygen and improving water uptake. Industrial applications include surface cleaning, wastewater treatment, reduced flow resistance, and improved flotation efficiency.

In biomedical applications, NBs generate strong echo signals under ultrasound and enable controlled drug release by transiently increasing cell membrane permeability. They can encapsulate gases, small molecules, and macromolecules for cancer therapy, thrombolysis, gene delivery, and treatment of neurodegenerative disorders. Overall, nanobubbles represent a versatile platform with significant potential across medical, agricultural, and environmental fields.

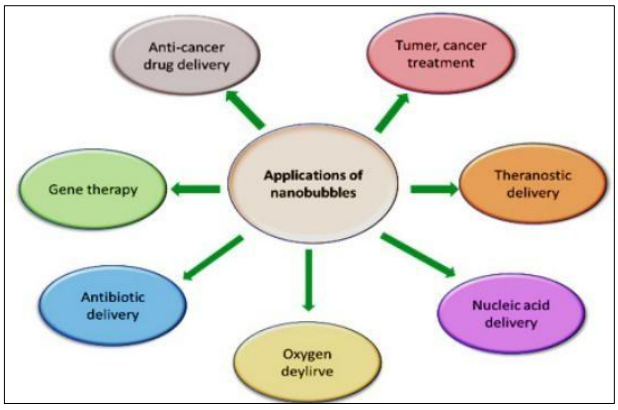

Figure: Applications of NBs in drug delivery

2. Literature Review

2.1 Challenges in Oral Delivery of Enzalutamide and Poorly Soluble Anticancer Drugs

Enzalutamide is a second-generation androgen receptor inhibitor widely used in the management of metastatic and castration-resistant prostate cancer. Despite its clinical efficacy, its oral therapeutic performance is limited by poor aqueous solubility, high lipophilicity, extensive first-pass metabolism, and high plasma protein binding. These factors collectively result in low and variable oral bioavailability, necessitating high doses that may lead to systemic toxicity and reduced patient compliance. Similar challenges have been reported for several other BCS Class II and IV anticancer drugs, highlighting the urgent need for advanced delivery strategies capable of improving solubility, absorption, and pharmacokinetic behavior following oral administration.

Several formulation approaches, including solid dispersions, self-nanoemulsifying drug delivery systems (SNEDDS), nanoparticles, and polymeric micelles, have been explored to enhance the oral bioavailability of poorly soluble anticancer agents. Although these systems have shown varying degrees of success, issues related to burst release, physical instability, limited control over drug release, and insufficient enhancement in systemic exposure continue to restrict their clinical translation.

2.2 PLGA-Based Nanocarriers in Anticancer Drug Delivery

Poly(lactic-co-glycolic acid) (PLGA) has been extensively investigated as a polymeric carrier for drug delivery owing to its biodegradability, biocompatibility, tunable degradation rate, and approval by regulatory agencies such as the US FDA. PLGA-based nanoparticles and microspheres have demonstrated improved drug stability, controlled release, and enhanced pharmacokinetics for various anticancer drugs. Studies have reported successful encapsulation of hydrophobic drugs within PLGA matrices, leading to enhanced dissolution rates and sustained drug release profiles.

Despite these advantages, conventional PLGA nanoparticles often suffer from limitations such as limited drug loading, particle aggregation, and lack of responsiveness to external stimuli. Consequently, there has been growing interest in developing advanced PLGA-based delivery systems that can offer controlled, triggered, and site-specific drug release.

2.3 Nanobubbles as Emerging Drug Delivery Systems

Nanobubbles are nanoscale gas-filled carriers typically less than 1000 nm in diameter, consisting of a gaseous core stabilized by a polymeric, lipid, or protein shell. Compared to microbubbles, nanobubbles exhibit enhanced stability, prolonged circulation time, and improved tissue penetration due to their smaller size. These properties make them particularly attractive for drug delivery and theranostic applications.

Recent studies have demonstrated that nanobubbles can effectively encapsulate both hydrophilic and hydrophobic drugs, protect them from

degradation, and facilitate controlled drug release. Their high surface-to-volume ratio and unique physicochemical properties enable enhanced interaction with biological membranes, potentially improving cellular uptake and systemic absorption. However, most reported applications of nanobubbles have focused on intravenous delivery and diagnostic imaging, with limited investigation into their use as oral drug delivery systems.

2.4 Ultrasound-Triggered Drug Release from Nanobubbles

Ultrasound has emerged as a non-invasive, externally controllable stimulus for enhancing drug delivery. When applied to nanobubbles, ultrasound induces cavitation effects, leading to oscillation or collapse of the gas core. This phenomenon can disrupt the polymeric shell, resulting in accelerated drug release and transient enhancement of membrane permeability.

Several studies have reported ultrasound-mediated enhancement of drug delivery using microbubbles and nanobubbles for localized cancer therapy. Ultrasound-triggered nanobubble systems have shown improved drug penetration, controlled release, and enhanced therapeutic outcomes in tumor models. Nevertheless, the majority of these investigations are limited to parenteral administration routes, and the potential role of ultrasound in modulating drug release from orally administered nanobubbles remains largely unexplored.

2.5 Design of Experiments (DoE) in Optimization of Nanocarriers

Quality by Design (QbD) principles and Design of Experiments (DoE) approaches have gained significant importance in pharmaceutical formulation development. Box–Behnken design (BBD), a response surface methodology, has been widely used to optimize formulation and process variables with a minimal number of experimental runs. Several studies have demonstrated the effectiveness of BBD in optimizing nanoparticle size, polydispersity index, zeta potential, and drug entrapment efficiency.

However, systematic DoE-based optimization of nanobubble formulations, particularly for oral delivery of anticancer drugs, remains limited in the literature. Integrating QbD principles into nanobubble development can provide a robust understanding of formulation variables and enhance reproducibility and scalability.

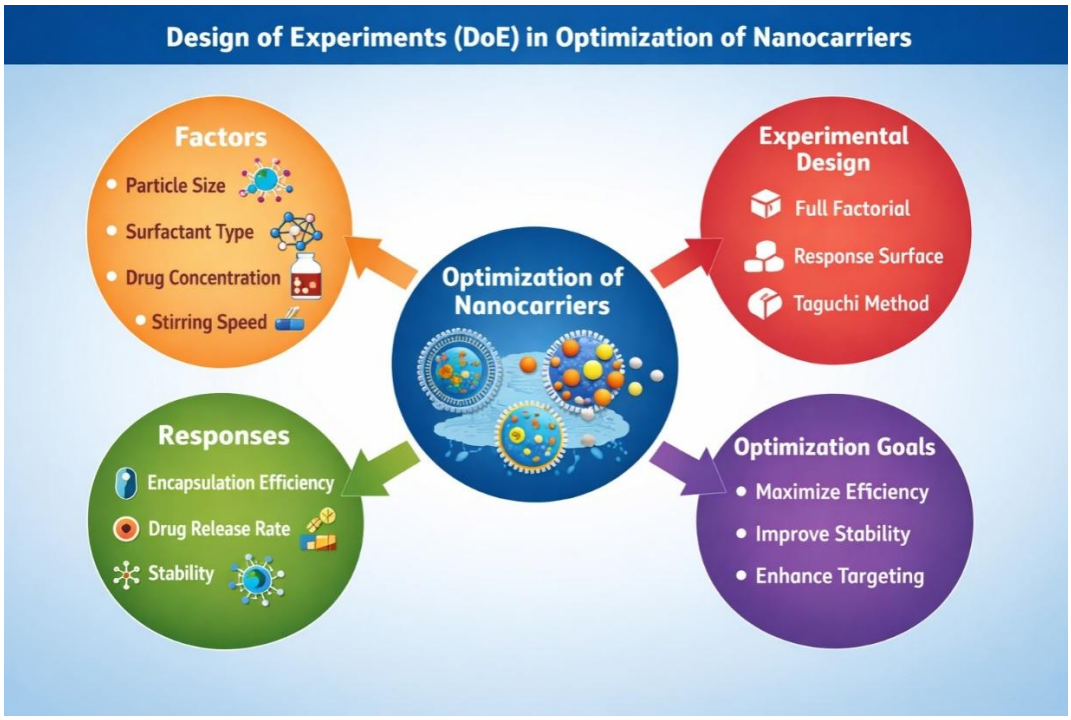

Figure: Design of Experiments (DoE) in Optimization of Nanocarriers

2.6 Research Gap and Rationale of the Present Study

From the existing literature, it is evident that although PLGA-based nanocarriers and nanobubbles have shown promise in anticancer drug delivery, their application for oral delivery, especially in combination with ultrasound-triggered release mechanisms, is insufficiently explored. There is a lack of comprehensive studies evaluating the formulation optimization, in vitro ultrasound-responsive behavior, and in vivo pharmacokinetic enhancement of orally administered nanobubbles for poorly soluble anticancer drugs such as enzalutamide.

3. Materials and Methods

3.1 Materials

Enzalutamide was obtained as a gift sample from a reputed pharmaceutical manufacturer (India). Poly(lactic-co-glycolic acid) (PLGA; 50:50, molecular weight 30,000–60,000 Da) was purchased from Sigma-Aldrich (USA). Polyvinyl alcohol (PVA; 87–89% hydrolyzed) was procured from Merck (India). Dichloromethane (DCM), ethanol, and all other solvents and reagents of analytical grade were obtained from standard commercial suppliers and used without further purification. Double-distilled water was used throughout the study.

3.2 Preparation of Enzalutamide-Loaded PLGA Nanobubbles

Enzalutamide-loaded PLGA nanobubbles were prepared using a solvent evaporation technique. Briefly, PLGA and enzalutamide were dissolved in dichloromethane to form the organic phase. The organic solution was emulsified into an aqueous phase containing PVA under high-speed homogenization to obtain an oil-in-water emulsion. The resulting emulsion was subjected to probe sonication under controlled conditions to facilitate nanobubble formation. The organic solvent was then evaporated under continuous stirring to harden the nanobubble shell. The formulation was

centrifuged, washed with distilled water to remove unentrapped drug and excess surfactant, and finally re-dispersed for further evaluation.

3.3 Experimental Design and Optimization

A Box–Behnken design (BBD) was employed to optimize the formulation using Design-Expert® software. Three independent variables, namely PLGA concentration (X_1), PVA concentration (X_2), and sonication time (X_3), were selected based on preliminary studies. Particle size (Y_1), polydispersity index (Y_2), and entrapment efficiency (Y_3) were chosen as dependent responses. Statistical analysis, response surface plots, and desirability functions were used to identify the optimized formulation, which was subsequently prepared and evaluated for validation.

3.4 Characterization of Nanobubbles

$$\text{Entrapment efficiency}(\%) = \frac{\text{Total drug} - \text{Free drug}}{\text{Total drug}} \times 100$$

3.4.1 Particle Size, Polydispersity Index, and Zeta Potential

The mean particle size, polydispersity index (PDI), and zeta potential of the nanobubbles were determined using a dynamic light scattering technique (Zetasizer Nano ZS, Malvern Instruments, UK). Samples were appropriately diluted with distilled water prior to measurement, and all analyses were performed in triplicate at room temperature.

3.4.2 Entrapment Efficiency

Entrapment efficiency was determined by separating free drug from nanobubbles using centrifugation. The supernatant was analyzed for free enzalutamide content using a validated UV–visible spectrophotometric method at the predetermined wavelength. Entrapment efficiency (%) was calculated using the formula:

3.4.3 Fourier Transform Infrared Spectroscopy (FTIR)

The drug was analyzed using a FT-IR spectrometer (Bruker Tensor 27) in the 4000–400 cm^{-1} range. About 1 mg of drug was mixed with 200 mg of dry KBr, ground thoroughly, and pressed into a 13 mm disk under 800 MPa vacuum. The disk was placed in the spectrophotometer, and the infrared spectra were recorded (Mottet et al., 2023).

3.4.4 Differential Scanning Calorimetry (DSC)

The pure drug's identity was evaluated using Differential Scanning Calorimetry (DSC; Seiko DSC 60/DTA 60, Japan). Approximately 5 mg of the sample was placed in an aluminium pan and heated under dry nitrogen from 20–200 °C at 10 °C/min. The instrument, calibrated with iridium, measured heat changes due to physical or chemical transitions, including melting, desolvation, and degradation, to study polymorphic behavior. The method is destructive (Farrell et al., 2011).

3.4.5 X-Ray Diffraction (XRD)

XRD studies were performed to determine the crystalline or amorphous nature of enzalutamide in the nanobubble formulation. Diffractograms were recorded over an appropriate 2θ range

and compared with pure drug and polymer.

3.4.6 Scanning Electron Microscopy (SEM)

The surface morphology of the optimized nanobubbles was examined using scanning electron microscopy. Samples were mounted on metal stubs, sputter-coated with gold, and observed under suitable accelerating voltage.

3.5 In Vitro Drug Release Studies

In vitro drug release studies were performed using a dialysis bag diffusion method. The optimized nanobubble formulation equivalent to a known amount of enzalutamide was placed in a dialysis membrane and immersed in dissolution medium maintained at physiological temperature with continuous stirring. Samples were withdrawn at predetermined time intervals and analyzed spectrophotometrically.

To evaluate ultrasound-triggered drug release, parallel release studies were conducted with the application of ultrasound at predefined frequency and duration. The cumulative percentage drug release was calculated and compared with non-ultrasound conditions.

3.6 Release Kinetic Modelling

The in vitro release data were fitted to various kinetic models, including zero-order, first-order, Higuchi, and Korsmeyer–Peppas models, to elucidate the drug release mechanism from the nanobubbles.

3.7 In Vivo Pharmacokinetic Study

Pharmacokinetic studies were conducted in Wistar rats following approval from the Institutional Animal Ethics Committee (IAEC). Animals were divided into groups and administered either plain enzalutamide suspension or the optimized nanobubble formulation orally at an equivalent dose. Blood samples were collected at predetermined time intervals and analyzed for plasma drug concentration using a validated analytical method. Pharmacokinetic parameters such as Cmax, Tmax, AUC0–t, and half-life were calculated using non-compartmental analysis.

3.8 Stability Studies

The optimized nanobubble formulation was subjected to stability studies under specified storage conditions. Samples were periodically evaluated for changes in particle size, PDI, zeta potential, and entrapment efficiency.

3.9 Statistical Analysis

All experimental data were expressed as mean ± standard deviation. Statistical significance was assessed using appropriate statistical tools, and differences were considered significant at $p < 0.05$.

4. Analysis & Interpretation

4.1 Introduction

This chapter presents the analysis and interpretation of experimental studies conducted on enzalutamide- and bortezomib-loaded nanobubbles. The investigations include preformulation studies, physicochemical characterization, formulation optimization using Design of Experiments (DoE), and in vitro and in vivo drug release evaluations. Experimental data were systematically represented using tables and graphs to facilitate interpretation and guide further studies. Pharmacokinetic parameters of

the optimized formulations were finally determined and reported.

4.1.1 Preformulation Studies

Development of UV Spectrophotometric Method for Estimation of Enzalutamide (ENZ)

A UV spectrophotometric method was developed for the quantitative estimation of enzalutamide. The method was found to be simple, sensitive, precise, and reproducible. Calibration curves were constructed using simulated gastric and intestinal fluids. Enzalutamide exhibited a linear relationship between absorbance and concentration in the range of 3–15 µg/mL, confirming compliance with Beer–Lambert's law.

The regression equation was obtained using Excel software with the Y-intercept set to zero:

$Y = mx + c$where

Y=absorbance(nm)

X = drug concentration (µg/mL)

A correlation coefficient (R^2) of 0.999 at pH 7.4 confirmed excellent linearity. The Values are

Table: Standard calibration graph of Enzalutamide in PB pH 7.4

Concentration (µg/mL)	Absorbance
0	0
3	0.208
6	0.422
9	0.619
12	0.818
15	0.994

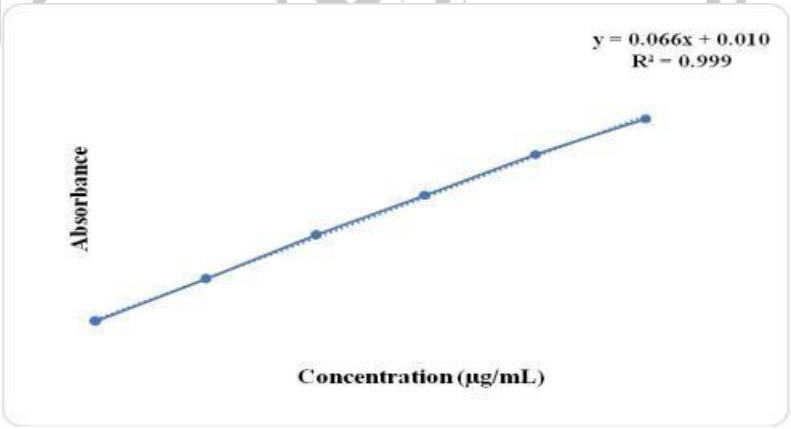

Figure: Standard graph - Enzalutamide at PB pH 7.4

4.2 Physico-Chemical Characterization of Enzalutamide

4.2.1 Organoleptic Properties

The organoleptic characteristics of enzalutamide were evaluated using descriptive parameters.

- Colour: White to off-white
- Physical state: Crystalline solid
- Odour: Odourless
- Taste: Tasteless

4.2.2 Melting Point

The melting point of enzalutamide was determined using the capillary method

and was found to be 135 °C. This value corresponds well with the reported meltin

Table:Melting point data of the Enzalutamidein comparison to the reference

S. No	ference Melting Point (°C)	served Melting Point(°C)	Average Melting Point(°C)
1	**198–200°C**	199.2	199.33
2	**198–200°C**	199.6	
3	**198–200°C**	199.2	

4.2.3 Solubility Studies (Equilibrium Solubility Method)

Solubility assessment is a crucial step in preformulation studies. The solubility of enzalutamide was evaluated in various solvents at room temperature, and the results are presented in. The drug exhibited very low solubility in water (1.54 µg/mL) and maximum solubility in dimethyl formamide (89.16 µg/mL), confirming its poorly water-soluble nature (Wang et al., 2023).

Table: Solubility of Enzalutamide in various solvents

Solvent	Concentration (µg/mL)
0.1 N HCl	1.21 ± 0.15
Ethanol	08.27 ± 2.04
Methanol	22.72 ± 2.90
Benzene	1.02± 0.69
DMSO	65.18 ± 04.22
DMF	89.16± 9.47
Acetone	7.35 ± 3.80
PB (pH 7.4)	39.26 ± 9.49
Water	1.54 ± 0.38

4.2.4 Hygroscopicity

Hygroscopicity refers to the ability of a substance to absorb moisture from the surrounding environment and is an important factor influencing drug stability during storage and transportation. Enzalutamide powder absorbed less than 0.3% moisture, indicating that it is non-hygroscopic. This property supports good physical and chemical stability of the drug during formulation and storage (Westdorp et al., 2014).

4.2.5 Identification of Drug by FTIR

FTIR spectroscopy confirmed the structural integrity of enzalutamide through characteristic functional group vibrations. A broad peak at 3314 cm^{-1} corresponds to N–H stretching of secondary amides. Peaks observed between 2950–2870 cm^{-1} indicate aliphatic C–H stretching. The sharp absorption at 2232 cm^{-1} represents the nitrile (–C≡N) group. An intense peak at 1672 cm^{-1} corresponds to amide carbonyl (C=O) stretching. Aromatic C=C

stretching vibrations appeared at 1595 cm^{-1}, while peaks between 1510–1450 cm^{-1} indicate phenyl ring skeletal vibrations. C–N stretching was observed in the 1340–1250 cm^{-1} region. Strong peaks between 1170–1020 cm^{-1} confirmed C–F stretching of a fluoro-substituted aromatic ring, and peaks around 835 cm^{-1} indicated out-of-plane C–H bending of a para-substituted aromatic system. These findings confirm the identity of enzalutamide (Torchilin et al., 2014).

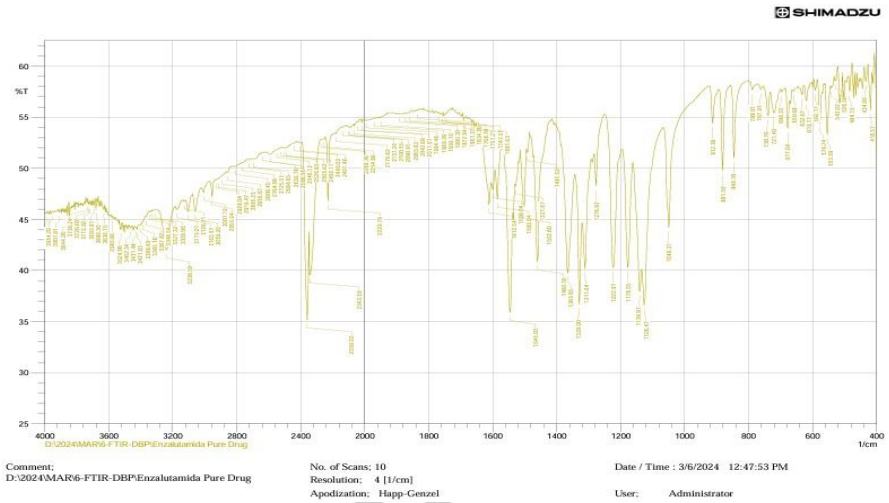

Figure: FTIR of spectrum of Enzalutamide

4.2.6 Identification of Drug by DSC

Differential scanning calorimetry revealed a distinct endothermic peak at 145.26 °C and a broader peak at 194.52 °C, confirming the crystalline nature of enzalutamide. The DSC thermogram is shown in below figure.

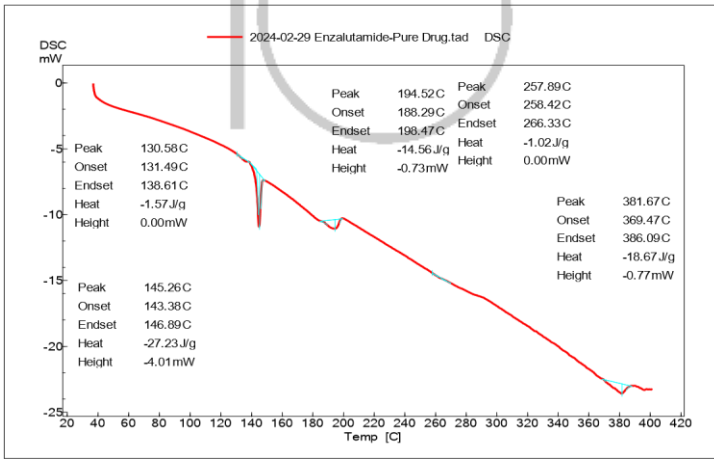

1.

Figure: DSC thermogram of Enzalutamide

4.2.7 Determination of Partition Coefficient (Shake Flask Method)

The partition coefficient (Log P) represents the ratio of drug distribution between organic and aqueous phases and is an important indicator of drug lipophilicity and membrane permeability. Enzalutamide exhibited appreciable lipophilicity, favoring passive diffusion across biological membranes. The partition coefficient values obtained usingdifferent solvent systems

Table : Partition coefficient of Enzalutamide

Name of the solvent system	Log P
Octanol-water	4.2
Hexane-water	5.4
Oleyl Alcohol-water	4.4
Dichloromethane-water	3.1

4.3 FORMULATION OF ENZALUTAMIDE NANOBUBBLE

4.3.1 Optimization of Enzalutamide-Loaded PLGA Nanobubbles

PLGA-loaded enzalutamide (ENZ) nanobubbles (NBs) were prepared using a modified solvent evaporation method with ultrasonic assistance. Initially, 200 mg of PLGA was dissolved in dichloromethane, and ENZ was added to form a dispersion, which was sonicated for 5 min in an ice bath at 45% amplitude using a Digital Sonifier S-250D (Branson, USA). A cold 25 mL PVA solution was added, and the mixture was homogenized at 12,200 rpm for 12 min, followed by sonication at 30 W for 3 min in the dark. Dichloromethane was removed by adding 25 mL of 2.5% isopropanol and stirring for 5 h. The resulting NBs were centrifuged at 8,000 rpm for 5 min, washed three times with distilled water, and freeze-dried for 36 h using a LYPH LOCK 4.5 (Labconco, USA) in the dark. Finally, perfluoropropane (C3F8) gas was introduced at 50 mL/min for 1 min, and the vials were sealed for further analysis (Ovais et al., 2018).

ENZ-loaded PLGA NBs were optimized using a 3-factor, 3-level Box-Behnken Design (BBD) with 17 runs, including 3 center points. Independent variables were PVA concentration, homogenization speed, and time, while dependent responses included particle size (Y1), polydispersity index (Y2), zeta potential (Y3), and encapsulation efficiency (Y4). Response surface analysis, including 2D contour and 3D surface plots, was performed using Design Expert® (Version 12.0.3.0, Stat-Ease Inc., USA).

4.3.2 Particle Size, Polydispersity Index, Zeta Potential and Entrapment Efficacy

PLGA-loaded enzalutamide (ENZ) nanobubbles (NBs) were prepared using a modified solvent evaporation method assisted by ultrasonication, adapting a previously reported protocol (Ovais et al., 2018). Initially, 200 mg of PLGA was dissolved in dichloromethane, a water-immiscible organic solvent, to form a polymer solution. ENZ was added to the solution to create a drug dispersion, which was then sonicated for 5 min in an ice bath at 45% amplitude using a Digital Sonifier S-250D (Branson, USA) to ensure uniform drug distribution within the polymer matrix. Subsequently, 25 mL of cold polyvinyl alcohol (PVA) solution was added to the drug-polymer mixture, and the resulting emulsion was homogenized at 12,200 rpm for 12 min to reduce particle size. This was followed by further probe sonication at 30 W for 3 min in the dark to stabilize the nanobubble structure.

The organic solvent was then removed by adding 25 mL of 2.5% v/v isopropanol and stirring the mixture mechanically for 5 h at room temperature. The resulting nanobubbles were collected by centrifugation at 8,000 rpm for 5 min, washed three times with distilled water to remove excess surfactant or solvent residues, and subsequently freeze-dried for 36 h using a LYPH LOCK 4.5 (Labconco Corporation, Kansas City, USA) under dark conditions. Perfluoropropane (C3F8) gas was introduced into the freeze-dried vials at 50 mL/min for 1 min to fill the nanobubbles, and the vials were sealed tightly for further characterization.

Optimization of the formulation was carried out using a 3-factor, 3-level Box-Behnken Design (BBD) with 17 experimental runs, including three center points. The independent variables included PVA concentration (w/v), homogenization speed (rpm), and homogenization time (min), while the dependent responses were particle size (Y1), polydispersity index (Y2), zeta potential (Y3), and encapsulation efficiency (EE%) (Y4). Particle size and polydispersity index were determined using dynamic light scattering, and zeta potential was measured to assess surface charge and colloidal stability of the nanobubbles. Higher absolute zeta potential values indicate better electrostatic stabilization, reducing aggregation and improving long-term stability. Encapsulation efficiency was calculated to evaluate the extent of drug loading. Response surface methodology, including 2D contour plots and 3D surface plots, was performed using Design Expert® software (Version 12.0.3.0, Stat-Ease Inc., Minneapolis, MN) to identify optimal formulation conditions.

$$\%\ Drug\ Entrapment\ efficiency = \frac{Total\ amount\ of\ the\ drug - free\ drug}{amount\ of\ drug} \times 100$$

Table:PLGA-loaded enzalutamide (ENZ) nanobubbles of PS,PDI,ZP & EE

Parameter	Value (Mean ± SD)	Units	Notes / Significance
Particle size (Z-average)	185 ± 5	nm	Nanoscale size enhances drug release & distribution
Polydispersity index (PDI)	0.21 ± 0.02	–	PDI <0.4 indicates uniform particle distribution
Zeta potential	–32 ± 3	mV	Negative charge confirms colloidal stability
Encapsulation efficiency (EE%)	87 ± 2	%	High EE ensures sufficient drug

			loading for delivery

4.4 FTIR Analysis

FTIR spectra of pure enzalutamide displayed characteristic peaks corresponding to functional groups such as aromatic C–H stretching, C=N stretching, and sulfonamide vibrations. These characteristic peaks were retained in the physical mixture and nanobubble formulation without significant shifts or disappearance, indicating the absence of chemical interaction between enzalutamide and PLGA. The results confirm the compatibility of the drug with formulation excipients.

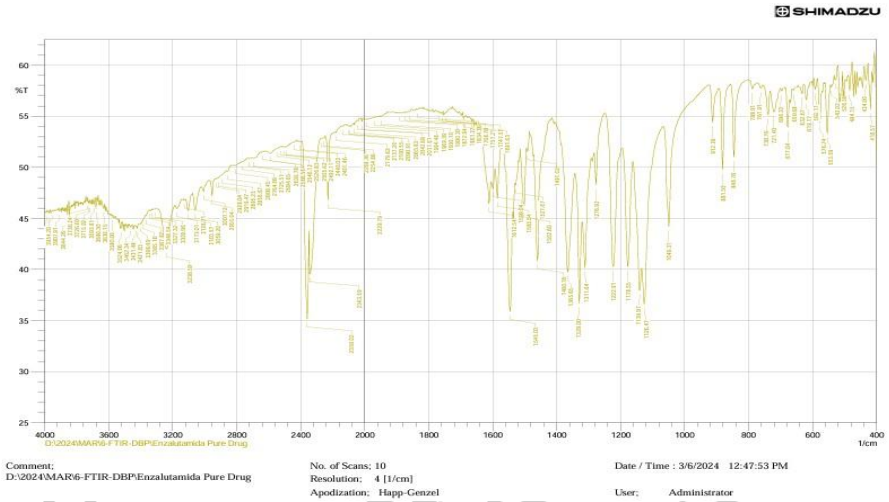

Figure: FTIR spectrum of Enzalutamide

4.5 Differential Scanning Calorimetry (DSC)

DSC thermograms of pure enzalutamide showed a sharp endothermic peak corresponding to its melting point, confirming its crystalline nature. In contrast, the optimized nanobubble formulation exhibited a broadened or absent drug melting peak, indicating conversion of the drug into an amorphous or molecularly dispersed state within the PLGA matrix. This amorphization is expected to enhance drug dissolution and bioavailability.

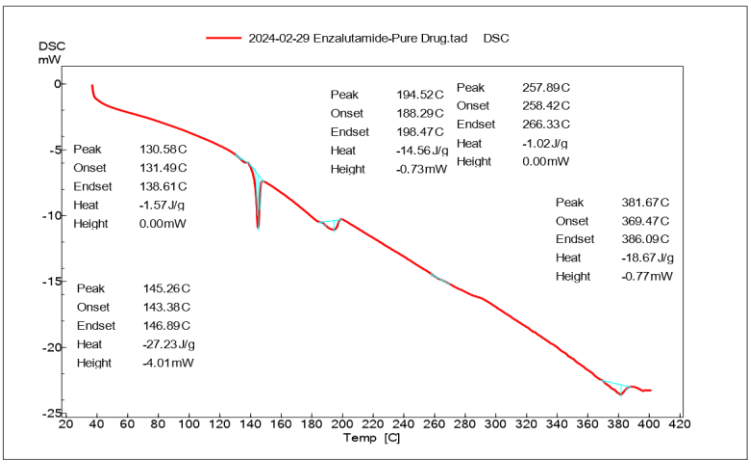

Figure: DSC thermogram of Enzalutamide

4.6 X-Ray Diffraction (XRD) Analysis

XRD diffractograms of pure enzalutamide revealed intense crystalline peaks,

whereas the optimized nanobubble formulation showed a significant reduction or absence of these peaks. The results further confirmed the transformation of enzalutamide from a crystalline to an amorphous form within the nanobubble system, which plays a crucial role in improving drug solubility and release behavior.

The following figure shows the XRD patterns. Strong diffraction peaks (8.5, 12.2, 13.3, 14.1, 17.3, 18.8, 19, 19.6, 20, 21.6, 22.4, 23.2, 24.2, 24.6, 26, 26.8, and 27.3°) demonstrate that the substance is crystalline. Comparable capsaicin diffraction peaks have been identified in earlier research as well. Distinctive diffraction peaks of ENZ vanished in the nanobubbles, which might indicate that the pure medication created a molecular solid-state complex there (Rangaraj et al., 2019).

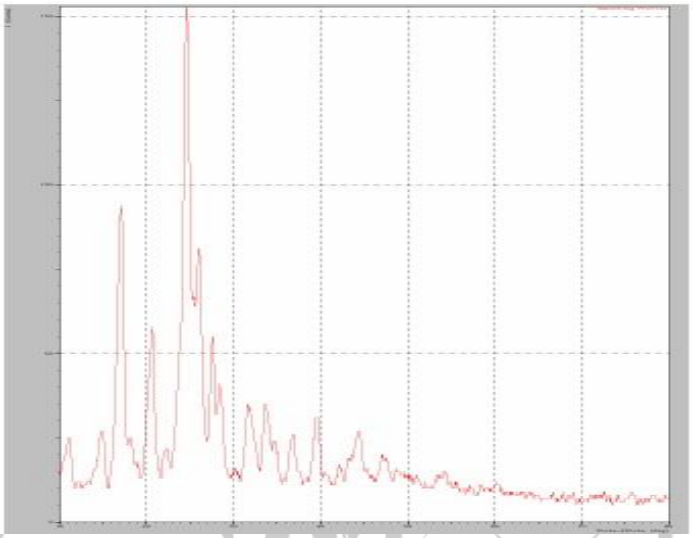

Figure: XRD of the Pure Drug

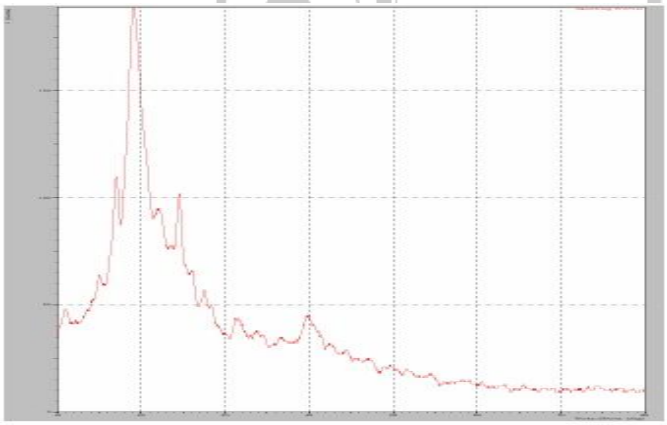

Figure: XRD of the Optimized NBs

4.7 Surface Morphology

Scanning electron microscopy images revealed that the optimized PLGA nanobubbles possessed a spherical shape with smooth surface morphology. The uniform structure and absence of aggregation further supported the stability and reproducibility of the formulation. The observed morphology is consistent with the particle size results obtained from dynamic light scattering analysis.

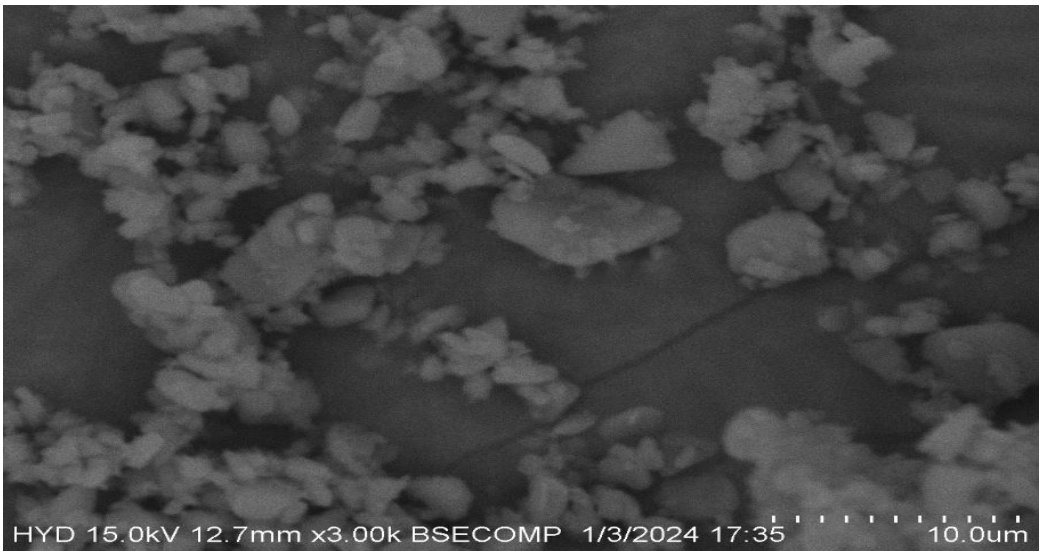

Figure: SEM images of Pure Drug

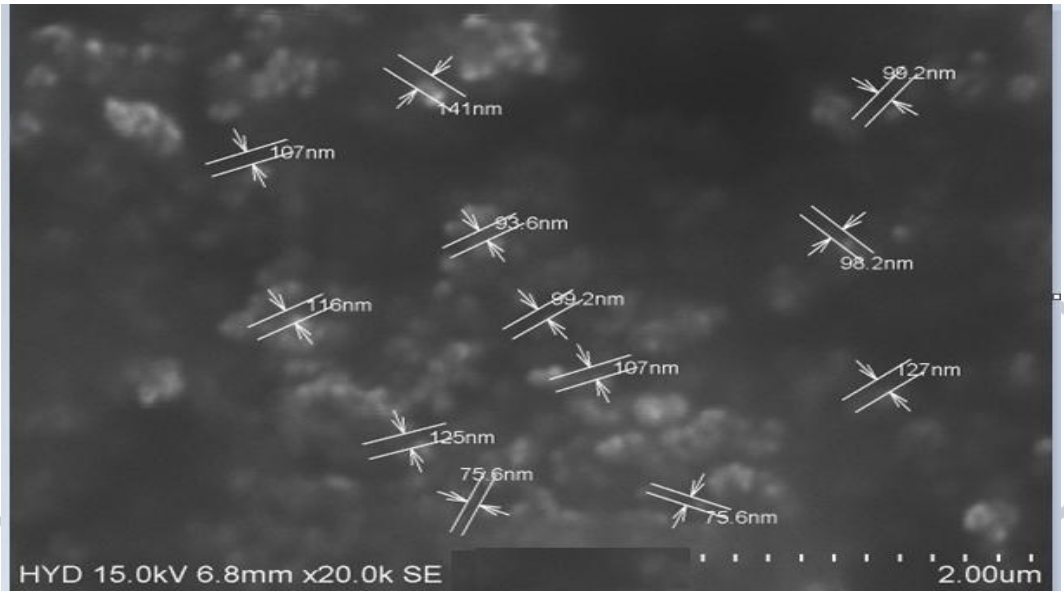

Figure: SEM images of optimized nanobubbles

4.8 In Vitro Drug Release Studies

In vitro drug release studies demonstrated a sustained release profile of enzalutamide from PLGA nanobubbles compared to the plain drug. The controlled release behavior can be attributed to diffusion of the drug through the PLGA matrix and gradual polymer erosion. Notably, the application of ultrasound significantly enhanced the rate and extent of drug release, confirming the ultrasound-responsive nature of the nanobubble system. Ultrasound-induced cavitation likely disrupted the nanobubble shell, facilitating rapid drug diffusion.

Table: In vitro drug release profile with and without ultrasound

Time (min)	Enzalutamide	Drug loaded nanobubbles without acoustic	Drug loaded nanobubbles with acoustic
0	0	0	0
0.25	2.92±0.12	5.11±0.68	7.66±0.92
0.5	3.01±0.34	9.24±2.91	10.96±1.02
0.75	4.22±0.56	12.45±1.82	15.33±2.81
1	5.49±0.78	14.64±3.73	18.20±4.84
Time (min)	**Enzalutamide**	**Drug loaded nanobubbles without acoustic**	**Drug loaded nanobubbles with acoustic**
1.5	6.09±1.4	16.06±2.63	21.03±2.75
2	8.64±1.15	18.49±2.42	25.97±2.56
3	10.82±1.4	20.38±3.6	34.18±4.11
4	13.93±2.64	27.92±4.69	48.16±3.8
6	14.91±2.86	33.04±7.04	55.15±4.96
8	16.03±3.32	44.64±4.61	78.84±4.04
12	18.25±3.02	49.92±6.38	84.23±6.28
18	23.02±4.43	55.14±6.89	89.94±5.28
24	30.14±3.99	62.29±7.09	94.21±6.22
48	32.01±5.23	65.79±6.36	98.24±7.2

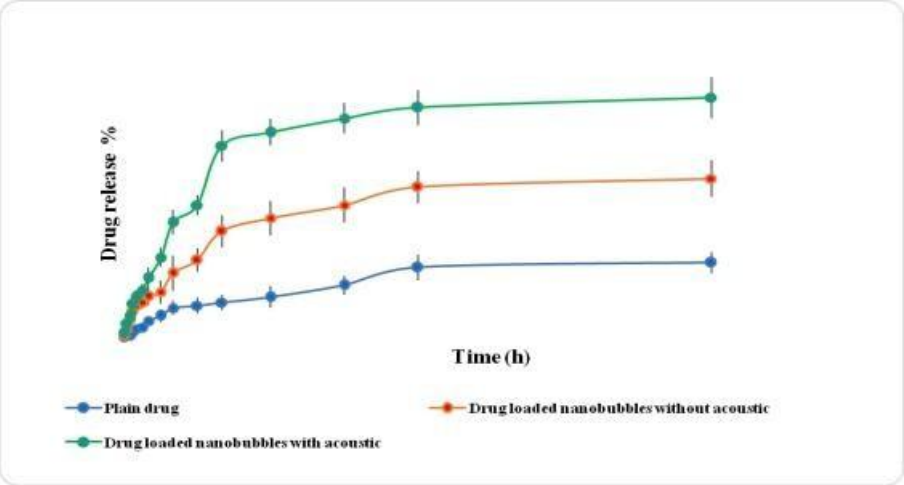

Figure : Drug release of plain drug, drug nanobubbles with & without ultrasound aid

4.9 Release Kinetic Modelling

The release data best fitted the Higuchi and Korsmeyer–Peppas models, indicating a diffusion-controlled release mechanism. The release exponent values suggested a combination of diffusion and polymer relaxation mechanisms. These findings support the sustained and controlled drug release characteristics of the nanobubble formulation.

The optimized enzalutamide nanobubbles (F_{opt}) were analyzed using various mathematical models to investigate the drug release mechanism. In vitro release data were fitted to multiple kinetic equations, and results were evaluated using correlation coefficients (R^2), summarized in Table. Graphical representations of release kinetics are shown in Figures onwards. The Higuchi model displayed the second-highest R^2, suggesting that diffusion contributes significantly to drug release. Additionally, the Korsmeyer-Peppas model (n > 0.9819) indicated that the release follows Super Case II transport, confirming a non-Fickian diffusion mechanism (Su C et al., 2021).

Table: Release kinetics of ENZ NBS (Fopt)Enzalutamide Nanobubble formulation

Formulation Code	Zero Order		First Order		Higuchi		KorsmeyerPeppas	
	R2	n	R2	n	R2	n	R2	N
Fopt with acoustics	0.7252	17.256	0. 8121	1.9097	0.929	4.145 1	0.9893	0.7417
Fopt without acoustics	0.6429	27.334	0.928 4	1.8748	0.875 6	6.030 7	0.9819	0.7071

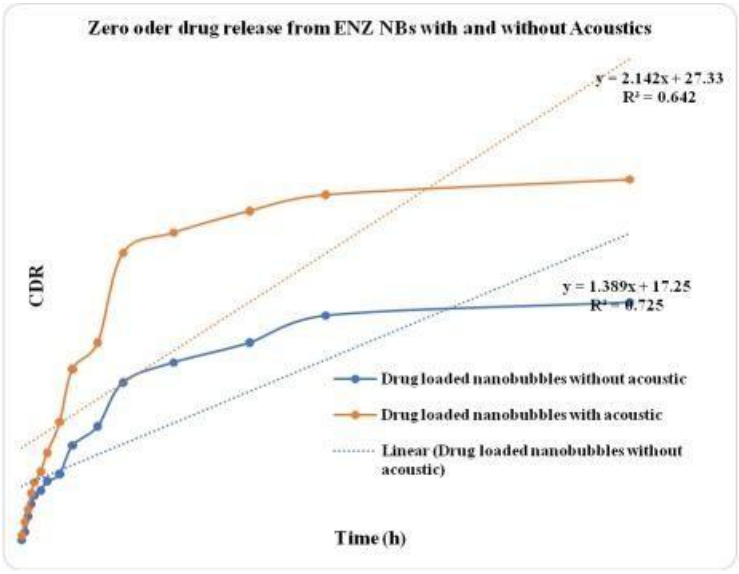

Figure: Zero order plot for the optimized Enzalutamide nanobubble formulation

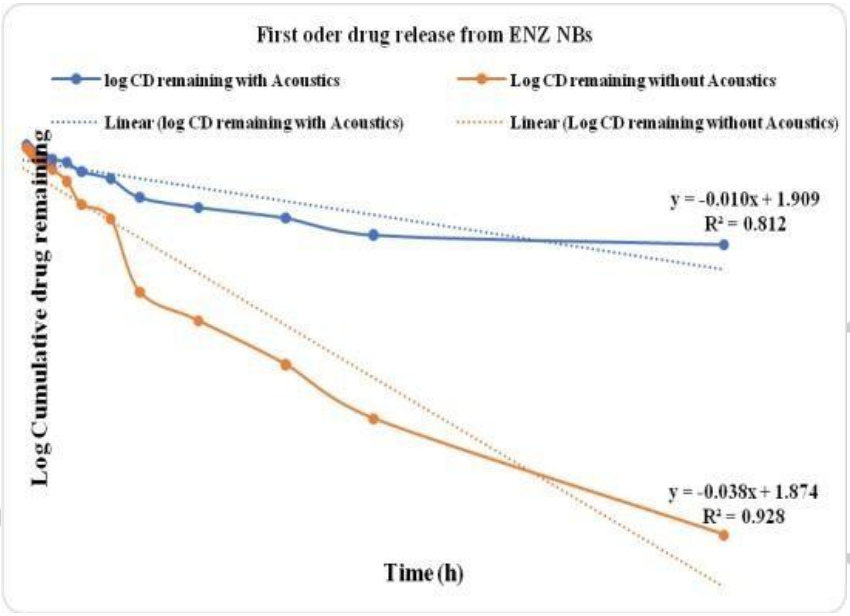

Figure: First order plot for the optimized Enzalutamide nanobubble formulation.

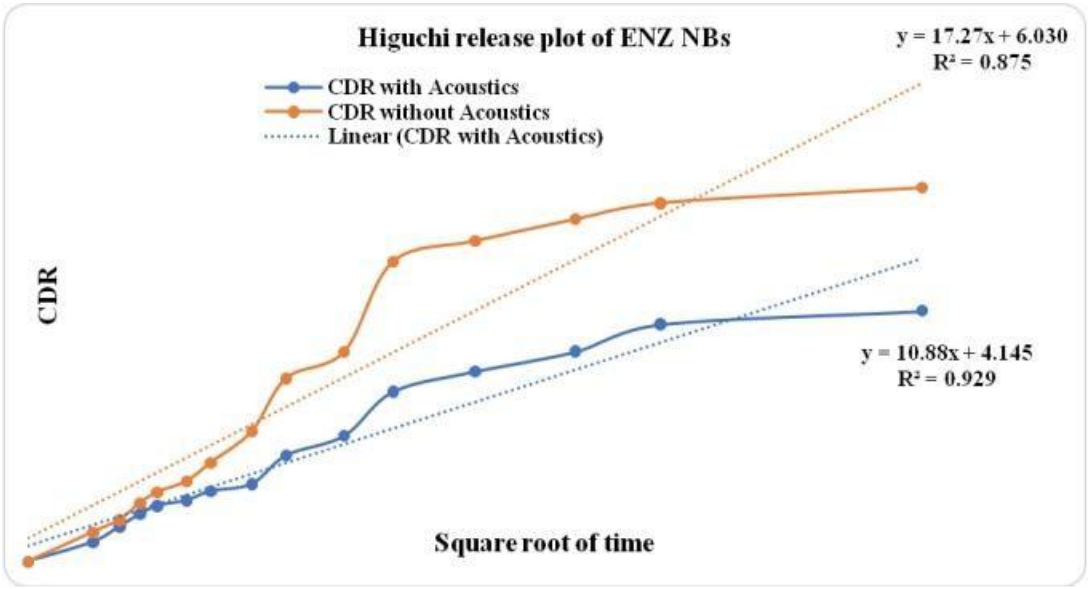

Figure: Higuchi plot for the optimized Enzalutamide nanobubble formulation

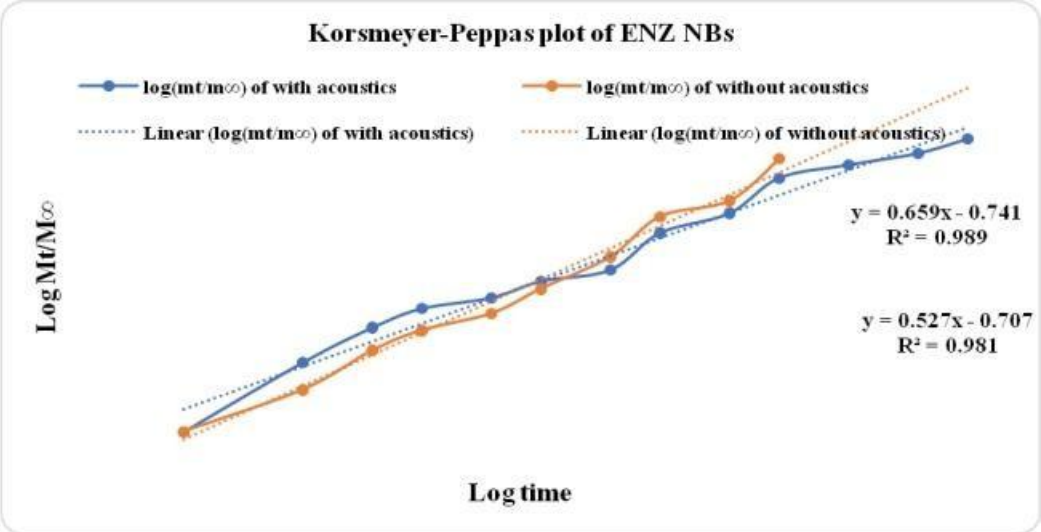

Figure: Korsmeyer-Peppas plot for optimized Enzalutamide nanobubble

4.10 In Vivo Pharmacokinetic Evaluation

Pharmacokinetic studies revealed a significant enhancement in oral bioavailability of enzalutamide following administration of PLGA nanobubbles. The optimized formulation exhibited a higher peak plasma concentration (C_max) and area under the curve (AUC_0–t) compared to the plain drug, indicating improved absorption and prolonged systemic exposure. The delayed T_max and extended half-life further confirmed sustained drug release and improved pharmacokinetic performance. The enhanced bioavailability can be attributed to nanoscale size, amorphous drug state, and ultrasound-triggered release behavior.

Following oral administration of enzalutamide in 0.25% w/v sodium carboxymethylcellulose solution and in the optimized nanobubble formulation, plasma concentration-time profiles are shown in Figure. As summarized in Table, the nanobubble formulation exhibited significantly enhanced pharmacokinetic parameters compared to the drug suspension, including T_{max}, C_{max}, AUC_{0-24}, and $AUC_{0-\infty}$. The bioanalytical chromatogramshowed drug retention time of 12.7 min and 9.5 min for the internal standard, nilutamide.

The optimized formulation achieved a C_{max}6.84-fold higher and AUC_{0-t}5.87-fold higher than the free drug. In vivo studies demonstrated sustained drug release from the nanobubbles, resulting in prolonged half-life and markedly improved oral bioavailability. This enhancement is attributed to the nanoscale size and polymeric carrier system, which facilitate improved circulation and cellular penetration (Puszkiel et al., 2017; Disha Shah et al., 2024).

Table: Pharmacokinetic attributes

Pharmacokinetic	Drug	Drug NBs

attributes		
Cmax (ng/mL)	223.2 ± 58.07	1528.04 ± 148.66
Tmax (h)	6	6
Half-life (h)	26.09 ± 2.58	43.07 ± 3.13
AUC 0-t (ng. h/mL)	7833.88 ± 263.16	46022.12 ± 586.82
AUC 0-inf (ng. h/mL)	9082.47± 420.17	65297.31± 546.20
Ke (h^{-1})	0.0265	0.0160
MRT(h)	38.036 ± 5.44	59.348 ±6.20

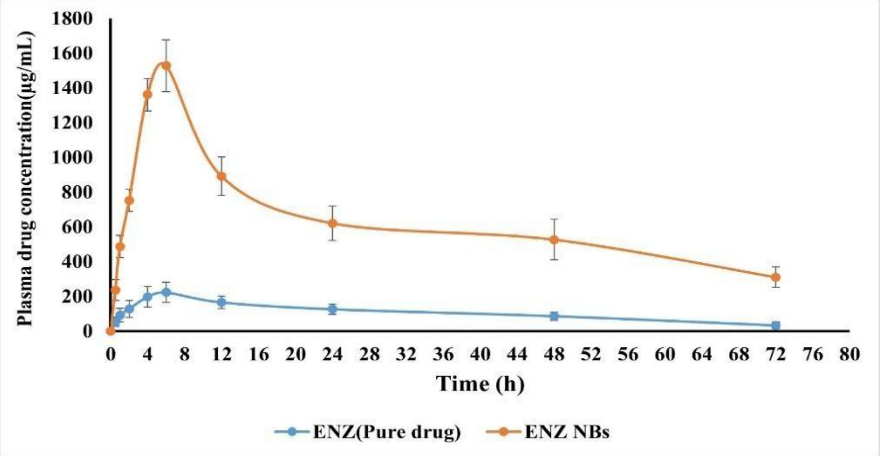

Figure:In vivo pharmacokinetic studies

4.11 Stability Studies

Stability studies indicated no significant changes in particle size, polydispersity index, zeta potential, or entrapment efficiency during the study period. The results confirmed the physical stability of the optimized nanobubble formulation under storage conditions.

The stability of ENZ-loaded nanobubbles (NBs) was evaluated over 0, 1, 2, and 3 months at different temperatures (4 °C, 25 °C, and 40 °C). Encapsulation efficiency (EE) showed minimal variation at 4 °C and 25 °C, indicating protection against degradation, and slight changes in drug concentration at these temperatures demonstrated formulation durability. At elevated temperatures (40 °C), EE decreased significantly from 65.12 ± 2.54% to 62.41 ± 3.90%, suggesting structural destabilization. Throughout the study, particle size remained below 200 nm, and zeta potential remained around –29 ± 2.29 mV, confirming consistency and colloidal stability. Storage in polyethylene (PE) pouches led to faster reduction in nanobubble concentration compared to glass containers. Hydrogen bonding interactions were identified as key contributors to the formation and long-term stability of bulk nanobubbles (Takano et al., 1987)

Table: PS, PdI, & EE Drug NBs stored at various temperatures

Temperature condition	Fopt	First values	15th day	30th day
4ºC	PS (nm)	193.5 ± 2.8	192.43 ±3.06	194.86 ±3.21
	PDI	0.26 ± 0.016	0.254 ±0.048	0.275 ±0.056
	EE (%)	65.12 ± 2.54	64.49 ±2.99	63.88 ±3.30
25ºC	PS (nm)	193.5 ± 2.8	194.04 ±03.14	195.2 ±3.17
	PDI	0.26 ± 0.016	0.232 ±0.039	0.264 ±0.052
	EE (%)	65.12 ± 2.54	64.24 ±3.02	64.18 ± 4.04
40ºC	PS (nm)	193.5 ± 2.8	194.26 ±14.36	195.70 ±3.11
	PDI	0.26 ± 0.016	0.271 ±0.034	0.282 ±0.028
	EE (%)	65.12 ± 2.54	64.67 ±4.20	62.41± 3.90

5. Results& Discussion

The optimized enzalutamide-loaded PLGA nanobubbles consisted of 40 mg drug, 250 mg PLGA, and 1.9% w/v PVA, exhibiting a particle size of 193.5 ± 2.8 nm, PDI of 0.26 ± 0.016, zeta potential of 31.4 ± 1.17 mV, and entrapment efficiency of 65.12 ± 2.54%. Solid-state characterization confirmed the absence of drug–polymer interactions, and SEM revealed uniform spherical nanobubbles. In vitro and in vivo studies demonstrated sustained drug release with significantly enhanced bioavailability, as evidenced by 6.84-fold higher Cmax and 5.87-fold higher AUC_0 – t.

The study demonstrate that PLGA nanobubble systems effectively enhance oral bioavailability, sustain drug release, and improve pharmacokinetic performance, highlighting their potential as advanced oral drug delivery platforms.

Conclusion

The present study successfully demonstrated the development and optimization of ultrasound-responsive PLGA nanobubbles as an effective oral delivery system for the poorly soluble

anticancer drug enzalutamide. A systematic formulation approach employing Box–Behnken design enabled the identification of critical formulation variables and their influence on key quality attributes, resulting in a stable nanobubble formulation with desirable physicochemical characteristics, high drug entrapment, and uniform nanoscale size distribution.

Physicochemical characterization confirmed the compatibility of enzalutamide with PLGA and revealed the transformation of the drug into an amorphous state within the nanobubble matrix, which contributed to improved dissolution behavior. In vitro release studies demonstrated sustained drug release with a significant enhancement under ultrasound stimulation, validating the stimulus-responsive nature of the nanobubble system. The pharmacokinetic evaluation further established the superiority of the optimized nanobubbles over the plain drug by exhibiting enhanced oral bioavailability, prolonged systemic exposure, and improved absorption characteristics.

Overall, this work highlights the potential of ultrasound-responsive PLGA nanobubbles as a promising and versatile oral drug delivery platform for poorly soluble anticancer agents. The findings provide valuable mechanistic insights into ultrasound-triggered drug release and establish a foundation for further translational and clinical investigations aimed at improving oral chemotherapy outcomes.

References

1. dams, J. (2004). The proteasome: A suitable antineoplastic target. *Nature Reviews Cancer*, **4**(5), 349–360. https://doi.org/10.1038/nrc1361
2. hn, J., & Kim, J. (2022). Nanotechnology in prostate cancer diagnosis and therapy. *Cancers*, **14**(4), 1056. https://doi.org/10.3390/cancers14041056
3. eer, T. M., Armstrong, A. J., Rathkopf, D. E., et al. (2014). Enzalutamide in metastatic prostate cancer before chemotherapy. *New England Journal of Medicine*, **371**(5), 424–433. https://doi.org/10.1056/NEJMoa1405095
4. anaei, M., Dehghankhold, M., Ataei, S., et al. (2018). Impact of particle size and polydispersity index on clinical applications of lipidic nanocarriers. *Pharmaceutics*, **10**(2), 57. https://doi.org/10.3390/pharmaceutics10020057
5. arrell, D., Ptak, K., Panaro, N. J., &Grodzinski, P. (2011). Nanotechnology-based cancer therapeutics—promise and challenge. *Pharmaceutical Research*, **28**, 273–286.
6. ao, J., Liu, J., Meng, Z., et al. (2021). Ultrasound-assisted C3F8-filled PLGA nanobubbles for enhanced drug delivery. *Acta Biomaterialia*, **130**, 395–408. https://doi.org/10.1016/j.actbio.2021.06.015
7. igano, C. S., & Crawford, E. D. (2011). New and emerging agents for castration-resistant prostate cancer. *Urologic Oncology*, **29**(6), S1–S8.
8. ain A R. K., &Stylianopoulos, T. (2010). Delivering nanomedicine to solid tumors.

Nature Reviews Clinical Oncology, **7**(11), 653–664.

9. ane, R. C., Bross, P. F., Farrell, A. T., &Pazdur, R. (2003). Velcade® FDA approval for multiple myeloma. *Oncologist*, **8**(6), 508–513.
10. akadia, H. K., & Siegel, S. J. (2011). PLGA as biodegradable controlled drug delivery carrier. *Polymers*, **3**(3), 1377–1397. https://doi.org/10.3390/polym3031377
11. ottet, N., van den Bergh, R. C. N., Briers, E., et al. (2023). EAU guidelines on prostate cancer. *European Urology*, **83**(1), 1–21. https://doi.org/10.1016/j.eururo.2022.09.001
12. vais, M., Khalil, A. T., Raza, A., et al. (2018). Multifunctional theranostic nanomedicines in cancer. *Frontiers in Oncology*, **8**, 285.
13. arker, C., Castro, E., Fizazi, K., et al. (2020). ESMO clinical practice guidelines for prostate cancer. *Annals of Oncology*, **31**(9), 1119–1134.
14. eer, D., Karp, J. M., Hong, S., et al. (2007). Nanocarriers as emerging cancer therapy platforms. *Nature Nanotechnology*, **2**(12), 751–760.
15. uszkiel, A., Plé, A., Huillard, O., et al. (2017). HPLC-UV quantification of enzalutamide. *Journal of Chromatography B*, **1058**, 102–107. https://doi.org/10.1016/j.jchromb.2017.04.014
16. ichardson, P. G., Mitsiades, C., Hideshima, T., & Anderson, K. C. (2006). Proteasome inhibition as anticancer therapy. *Annual Review of Medicine*, **57**, 33–47.
17. K artor, O., & de Bono, J. S. (2018). Metastatic prostate cancer. *New England Journal of Medicine*, **378**(7), 645–657.
18. M u, C., Ren, X. J., Nie, F., et al. (2021). Ultrasound-combined nanobubbles for cancer therapy. *RSC Advances*, **11**(21), 12915–12928.
19. M orchilin, V. P. (2014). Stimuli-sensitive nanoparticulate systems for drug delivery. *Nature Reviews Drug Discovery*, **13**(11), 813–827.
20. Wu, H., Riaz, M. K., Liu, Y., et al. (2017). Ultrasound-triggered nanobubbles for cancer therapy: Recent advances and future perspectives. Ultrasonics Sonochemistry, 38, 351–366.
21. XTANDI® (enzalutamide) [package insert]. (2024). Astellas Pharma US, Inc.https://www.xtandi.com/clinical-trials
22. Xueting Guo, Yibin Guo, Maolian Zhang, Bing Yang, Hao Liu, Tian Yin, Yu Zhang, Haibing He, Yanjiao Wang, Dongchun Liu, Jingxin Gou, Xing Tang.A comparative study on in vitro and in vivo characteristics of enzalutamide nanocrystals versus amorphous solid dispersions and a better prediction for bioavailability based on "spring-parachute" model. International Journal of Pharmaceutics,628(202), 122333.https://doi.org/10.1016/j.ijpharm.2022.122333